SIAM J. Appl. Math.
Vol. 0, No. 0, pp. 000–000

RESCUE OF THE QUASI-STEADY-STATE APPROXIMATION IN A MODEL FOR OSCILLATIONS IN AN ENZYMATIC CASCADE*

THOMAS ERNEUX† AND ALBERT GOLDBETER‡

We wish to dedicate this paper to the memory of L. A. Segel who contributed to many aspects of mathematical biology and for whom the quasi-steady-state hypothesis was a favorite topic of research

Abstract. A three-variable model describing the oscillatory activity of a cascade of enzyme reactions is analyzed. A quasi-steady-state approximation reduces the three equations to a system of two equations which admits only a stable steady state. This apparent failure of the quasi-steady-state approximation to describe the limit-cycle oscillations observed in the full, three-variable system is analyzed in detail. We first show that the oscillations occur in the full system provided the Michaelis constants are sufficiently small. We then develop a method for determining the correct limit for application of the quasi-steady-state approximation. The leading problem consists of two equations for a conservative oscillator, and a higher order analysis is required in order to determine the amplitude of the limit-cycle oscillations. Finally, we observe a good agreement when comparing exact numerical and approximate bifurcation diagrams.

Key words. enzyme reactions, limit-cycle oscillations, quasi-steady-state approximation, singular perturbation

AMS subject classifications. 34E05, 34E15, 92C45

DOI. 10.1137/060654359

1. Introduction.

The quasi-steady-state approximation (QSSA) of chemical kinetics is a mathematical way of simplifying the differential equations describing some chemical kinetic systems. This approximation is a powerful tool for analyzing the dynamics of enzymatic reactions [1, 2, 3] exhibiting a wide range of time scales. The QSSA often yields revealing analytic formulas, and it frequently circumvents problems of stiffness in the numerical integration of systems of differential equations. Originally devised by biochemists on the basis that enzymes as catalysts act with small concentrations compared to the concentrations of their substrates, the QSSA is now recognized as belonging to singular perturbation theory. Ideally, this theory provides a method for the correct use of the QSSA, but it is too complicated for general use. Various investigations of special cases, such as the Michaelis–Menten reaction [4, 5, 6], give some indications of the applicability of the QSSA. But further clarification is called for, especially since the QSSA is virtually unavoidable in introductory texts on chemical or biochemical kinetics [1, 2, 3, 7, 8]. Biological oscillations often exhibit different time or amplitude scales, and the QSSA is widely used to analyze excitability and limit-cycle oscillations in the phase plane (see [9, 10, 11], for biochemical examples). In this paper, we concentrate on a three-variable model for the oscillations in

*Received by the editors March 15, 2006; accepted for publication (in revised form) August 25, 2006; published electronically DATE.
http://www.siam.org/journals/siap/x-x/65435.html

†Optique Nonlinéaire Théorique, Université Libre de Bruxelles, Campus Plaine, C.P. 231, 1050 Bruxelles, Belgium (terneux@ulb.ac.be). The work of this author was supported by the Fonds National de la Recherche Scientifique (Belgium).

‡Unité de Chronobiologie Théorique, Université Libre de Bruxelles, Campus Plaine, C.P. 231, 1050 Bruxelles, Belgium (agoldbet@ulb.ac.be). The work of this author was supported by the European Union through the Network of Excellence BioSim, contract LSHB-CT-2004-005137, and by grant 3.4636.04 from the Fonds de la Recherche Scientifique Médicale (F.R.S.M., Belgium).

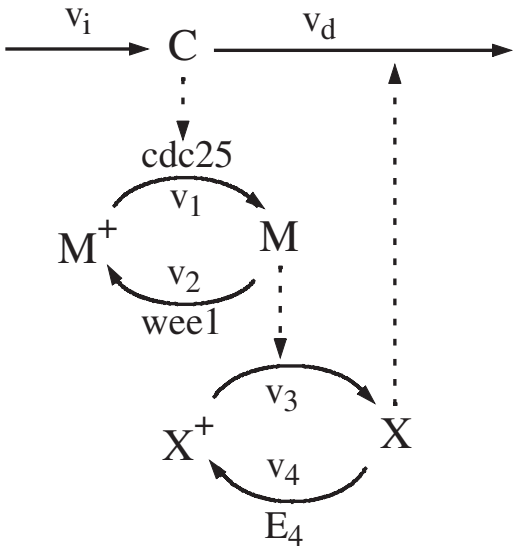

FIG. 1. *Bicyclic cascade model for the mitotic oscillator underlying the early cell cycle in amphibian embryos* [16, 17]. *Cyclin (C) is synthesized at a constant rate (v_i) and activates cdc*25 *phosphatase. The activated cdc*25 *phosphatase in turns activates cdc*2 *kinase (M) by dephosphorylating the inactive form (M^+). The activated cdc*2 *kinase is inactivated by the kinase wee*1. *In addition, a cyclin protease X is activated by cdc*2 *kinase and inactivated by an additional phosphatase (E_4). V_j ($j = 1 - 4$) denotes the effective maximum rate of each of the four converter enzymes; v_d denotes the maximum rate of cyclin degradation by protease X.*

the embryonic cell cycle and discover that the immediate application of the QSSA fails to describe these oscillations. Our main objective is to determine why the QSSA failed and how we may correctly use it in our problem.

Models for biochemical oscillations often contain one or more sigmoidal functions. Combined with positive and/or negative feedback loops, these functions allow the emergence of simple or complex oscillatory behavior. The sigmoidal dependence originates at the molecular level either from cooperative interactions in allosteric enzymes or from the phenomenon of zero-order ultrasensitivity in which two enzymes catalyzing opposite covalent modification reactions (e.g., phosphorylation-dephosphorylation) are saturated by their protein substrate [12]. While allosteric enzymes are abundant in metabolic regulation, covalent modification also plays an important role in biological signaling and cell regulation. Models for the oscillatory activity of allosteric enzymes have been studied analytically by taking advantage of the relatively large values of the allosteric constants [13, 14, 15]. However, the case of several enzymes working in a covalent modification cascade and exhibiting oscillatory activities has never been examined from an analytical point of view. In this paper, we consider a minimal model for biochemical oscillations underlying the embryonic cell cycle [16, 17]. See Figure 1. This model pertains to the situation encountered in early amphibian embryos, where the accumulation of cyclin suffices to trigger the onset of mitosis. In yeast and somatic cells, the mechanism involves additional checkpoints; see [2, 3, 18] and references therein. But what remain common to the various types of cell cycle mechanisms is the fact that they rely on the periodic activation of kinase cdc2 (also known as the cyclin-dependent kinase 1, cdk1). Cyclin activates the kinase cdc2, which promotes the degradation of cyclin. To produce oscillations, however,

activation and degradation cannot occur simultaneously and the negative feedback loop must be coupled to thresholds and time delays, which are naturally associated with phosphorylation-dephosphorylation cascades [16, 17].

The model is formulated in terms of the following three ordinary differential equations for the cyclin concentration C, the fraction of active cdc2 kinase M, and the fraction of active cyclin protease X [16, 17]:

$$\frac{dC}{dt} = v_i - v_d X \frac{C}{K_d + C} - k_d C, \tag{1}$$

$$\frac{dM}{dt} = V_{M1} \frac{C}{K_c + C} \frac{1 - M}{K_1 + 1 - M} - V_2 \frac{M}{K_2 + M}, \tag{2}$$

$$\frac{dX}{dt} = V_{M3} M \frac{1 - X}{K_3 + 1 - X} - V_4 \frac{X}{K_4 + X}. \tag{3}$$

In these equations, $1-M$ and $1-X$ represent the fractions of inactive cdc2 kinase and cyclin protease, respectively. v_i and v_d are the constant rate of cyclin synthesis and the maximum rate of cyclin degradation by protease X ($X = 1$), respectively. K_d and K_c denote the Michaelis constants for cyclin degradation and for cyclin activation of the cdc25 phosphatase acting on the phosphorylated form of the cdc2 kinase, respectively. k_d represents an apparent first-order rate constant related to nonspecific degradation of cyclin. The remaining parameters V_i and K_i ($i = 1$ to 4) denote the effective maximum rates and the Michaelis constants, respectively, for each of the enzymes E_i involved in the two cycles of phosphorylation-dephosphorylation. Moreover, the effective maximum rates $V_1(C)$ and $V_3(M)$ are given by $V_1 = V_{M1}C/(K_c + C)$ and $V_3 = V_{M3}M$.

The parameter K_d has been introduced to avoid the possibility that C becomes negative [16, 17]. For all our numerical solutions, however, we used $K_d = 0$ and found that C is always positive. Equation (1) with $K_d = 0$ is linear, and the nonlinearities necessary for the limit-cycle oscillations are given by the right-hand sides of (2) and (3). At steady state, the functions $M = M(C)$ and $X = X(M)$ obtained by setting the right-hand sides of (2) and (3) equal to zero are sigmoidal functions of M and X. The role of these functions for the oscillations is discussed in [16, 17]. Examples of limit-cycle oscillations for moderate and high values of V_{M1} and V_2 ($V_2/V_{M1} = 1/2$ fixed) are shown in Figure 2. They have been obtained by numerically solving (1)–(3). In Figure 2, top, the maximum rates V_{M1} and V_2 are moderate. The kinase M is activated as soon as C reaches a value close to 0.5. In Figure 2, bottom, the maximum rates V_{M1} and V_2 are large. In contrast to Figure 2, top, C remains close to 0.5. Time t, concentration C, and all parameters except the Michaelis constants have units as in [16, 17], where simulations are compared to experiments. We keep these equations in this form because they appear in all previous studies [16, 17, 30, 31].

We wish to describe the limit-cycle oscillations by using phase plane techniques. To this end, we propose to eliminate either M or X by using a QSSA. But, as we shall demonstrate, the reduced two-variable equations do no more exhibit limit-cycle oscillations. By using a singular perturbation method, we then determine the correct two-variable limit that allows us to recover sustained oscillatory behavior. This analysis involves two steps. We first show that the leading approximation of the limit-cycle solution satisfies a two-variable conservative system of equations such as the Lotka–Volterra equations of chemical kinetics [1]. This system gives the correct relation

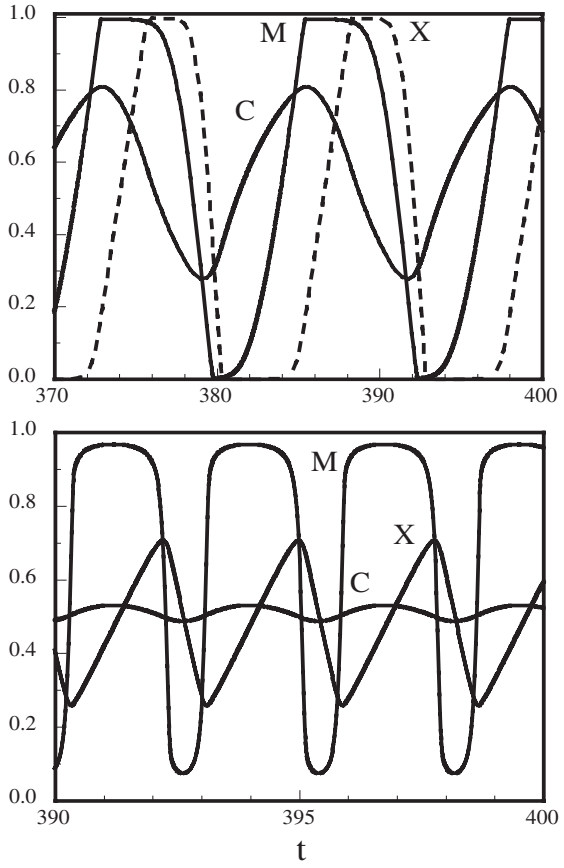

FIG. 2. *Limit-cycle oscillations in the enzymatic cascade model. M is dimensionless, C is measured in μM, and time t is measured in minutes. The values of the parameters are $K_j = K = 10^{-3}$ $(j = 1 - 4)$ and (in min^{-1}), $V_{M3} = 1$, $V_4 = 0.7$, $k_d = 0.25$; (in μM min^{-1}), $v_i = v_d = 0.25$; (in μM), $K_c = 0.5$, $K_d = 0$. Top: $V_{M1} = 3$ min^{-1} and $V_2 = 1.5$ min^{-1}; bottom: $V_{M1} = 3000$ min^{-1} and $V_2 = 1500$ min^{-1}.*

between the period and the amplitude of the oscillations. But in order to find how the amplitude changes with a given control parameter, a higher order analysis leading to a condition for bounded periodic solutions is needed. Similar singular perturbation techniques for particular Hopf bifurcation problems have been studied for chemical and biochemical relaxation oscillations [20], pulsating solidification fronts [21], and pulsating laser oscillations [24, 25].

The plan of the paper is as follows. In section 2, we show the failure of the standard QSSA and identify the source of the problem. Section 3 summarizes the results of our analysis, leading to the correct limit. The bifurcation diagram of the reduced two-variable equations is compared to the bifurcation diagram of the original three-variable equations. The main results are summarized in section 4. Mathematical details are given in appendices.

2. Failure of the QSSA. Equations (1)–(3) are too complicated for phase space analysis. A popular technique for simplifying the problem is to apply a QSSA for one of the dependent variables. This approximation (also called a pseudo-steady-state

hypothesis [26], steady-state assumption [27], or adiabatic elimination [28, 29]) is based on the assumption that the enzyme reacts so fast with the substrate that it can be taken as being in equilibrium, that is to say, $dM/dt \approx 0$ or $dX/dt \approx 0$. This approximation has been highly documented for the Michaelis–Menten reaction [1, 2, 3, 4, 5, 6] but has been used successfully for more complex systems exhibiting several enzymatic intermediates [2, 11]. The approximation is justified mathematically if a small parameter multiplies the time derivative of one of the dependent variables. This occurs in our problem if we consider the case of large values of both V_{M1} and V_2 (or, similarly, if we consider large values of V_{M3} and V_4). The proper way to apply the QSSA is to introduce the large parameter V defined as

$$V \equiv V_{M1} \tag{4}$$

and scale V_2 as

$$V_2 = V v_2, \tag{5}$$

where the coefficient v_2 is assumed to be an order one quantity. We may then factorize V in the right-hand side of (2) and rewrite this equation as

$$V^{-1}\frac{dM}{dt} = \frac{C}{K_c + C}\frac{1 - M}{K_1 + 1 - M} - v_2\frac{M}{K_2 + M}. \tag{6}$$

The coefficient of dM/dt is small because V is large. Thus, unless dM/dt is large, we may neglect this term and formulate the following algebraic equation for M and C:

$$\frac{C}{K_c + C}\frac{1 - M}{K_1 + 1 - M} - v_2\frac{M}{K_2 + M} = 0. \tag{7}$$

The QSSA is the assumption $V^{-1}dM/dt = 0$. Solving (7) for M and introducing $M = M(C)$ into (1) and (3) leads to two equations for only C and X. The two-variable problem represents a major simplification of our original three-variable equations, and we wonder if this reduced problem still admits limit-cycle oscillations. To this end, we examine the linear stability of the unique steady state $(C, X) = (C_s, X_s)$. We find that the coefficients of the characteristic equation for the growth rate σ are always positive. This means that $\mathrm{Re}(\sigma)$ is negative, implying stability of the steady state. A similar conclusion is obtained if we consider the case when V_{M3} and V_4 are large and eliminate the variable X.

We have thus found that a naive QSSA which allowed us to eliminate either M or X fails to describe the limit-cycle oscillations. But this approximation is nothing else than the leading term of an asymptotic solution and, like any asymptotic solution, it may admit different limits depending on the values of the other parameters in the problem. Returning to the original three-variable equations (1)–(3), we numerically investigate the behavior of the limit-cycle oscillations for progressively larger values of $V = V_{M1}$ and V_2 ($v_2 = V_2/V_{M1}$ fixed). We find that these oscillations persist only if we decrease the Michaelis constants K_j. The importance of these constants can be substantiated analytically by analyzing the Hopf bifurcation conditions in the double limit $V \to \infty$ and $K_j = K \to 0$ ($j = 1, 4$). The detailed analysis is given in Appendix A, where we show that the Hopf bifurcation point $K = K_H(V)$ scales like

$$K_H \sim V^{-1/2} \tag{8}$$

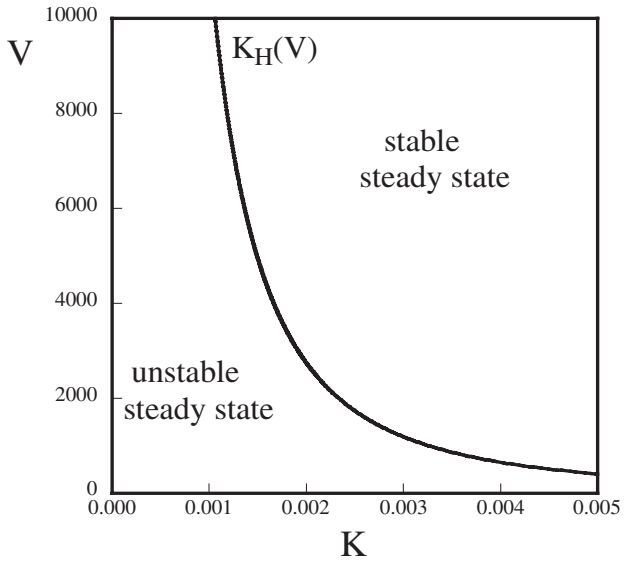

FIG. 3. *Hopf bifurcation line in the (K, V) parameter space. $V \equiv V_{M1}$ and $V_2 = V_{M1}/2$. The values of the other parameters are the same as in Figure 2. For progressively larger values of the maximum rate V, it is necessary to decrease the Michaelis constants (all equal to K) in order to keep the limit-cycle oscillations.*

as $V \to \infty$. Figure 3 shows the exact numerical Hopf bifurcation line for large values of V. It is in very good agreement with the approximation (47) derived in Appendix A. At a fixed value of V, the unique steady state undergoes a Hopf bifurcation at $K = K_H$, and the steady-state solution is unstable if $K < K_H$. From the Hopf conditions, we also learn that the frequency ω_H of the oscillations at the Hopf bifurcation point scales like

$$\omega_H \sim V^{1/4} \tag{9}$$

as $V \to \infty$, suggesting a short period oscillations for V large. We conclude that the QSSA based on the sole limit $V \to \infty$ cannot describe the oscillations unless we scale K as a $V^{-1/2}$ quantity and introduce a new time proportional to $V^{1/4}t$. In [16, 17], the value of V was much lower, allowing a larger K, for the observation of sustained oscillations.

3. Rescue of the QSSA. Phosphorylation-dephosphorylation cascades were already analyzed in the limit of small values of the Michaelis constants [19]. The difficulty here is that we need to scale both the maximum velocities and the Michaelis constants in order to describe the oscillations. Using the definitions (4) and (5), and motivated by the scaling laws (8) and (9), we introduce a small parameter ε, defined by

$$\varepsilon \equiv V^{-1/4}, \tag{10}$$

and scale the parameters V_2 and K_j $(j = 1 - 4)$ with respect to ε as

$$V_2 = \varepsilon^{-4} v_2 \text{ and } K_j = \varepsilon^2 k_j \ (j = 1 - 4). \tag{11}$$

In (11), v_2 and k_j are assumed to be order one coefficients. We also take into account (9) by introducing a new basic time T defined by

$$T \equiv \varepsilon^{-1} t. \tag{12}$$

Inserting (10)–(12) into (1)–(3) gives

$$\varepsilon^{-1} \frac{dC}{dT} = v_i - v_d X \frac{C}{K_d + C} - k_d C, \tag{13}$$

$$\frac{dM}{dT} = \varepsilon^{-3} \left[\frac{C}{K_c + C} \frac{1 - M}{\varepsilon^2 k_1 + 1 - M} - v_2 \frac{M}{\varepsilon^2 k_2 + M} \right], \tag{14}$$

$$\varepsilon^{-1} \frac{dX}{dT} = V_{M3} M \frac{1 - X}{\varepsilon^2 k_3 + 1 - X} - V_4 \frac{X}{\varepsilon^2 k_4 + X}. \tag{15}$$

Our QSSA now means the solution of these equations in the limit ε small. The analysis is long and tedious and is relegated to Appendix B. The results of our analysis are, however, simple and are summarized as follows for the case $K_d = 0$.

The leading approximation of the solution of (13)–(15) is described in terms of the variables M, U, and W, where U and W are defined as the deviations of C and X from their steady-state values

$$U \equiv \varepsilon^{-2}(C - C_0) \text{ and } W \equiv \varepsilon^{-1}(X - X_0). \tag{16}$$

In (16), C_0 and X_0 represent the steady-state values of C and X evaluated at $K_j = 0$ $(j = 1 - 4)$. They are defined as

$$C_0 \equiv \frac{K_c v_2}{1 - v_2} \text{ and } X_0 \equiv \frac{(v_i - k_d C_0)}{v_d}. \tag{17}$$

The leading order equations for M and W are then given by

$$F'(M) \frac{dM}{dT} = -v_d W, \tag{18}$$

$$\frac{dW}{dT} = V_{M3} M - V_4, \tag{19}$$

where

$$F(M) \equiv \frac{K_c v_2}{(1 - v_2)^2} \left[\frac{k_1}{1 - M} - \frac{k_2}{M} \right] \tag{20}$$

and

$$U = F(M). \tag{21}$$

Equations (18) and (19) form a conservative system of equations which admits a one-parameter family of periodic solutions. See Figure 4. For each point in the phase plane (W, M), there exists a closed orbit surrounding the center located at $(W, M) = (0, V_4/V_{M3})$. As the amplitude of the orbit increases, the period increases. The orbit becomes more and more rectangular and spends most of its time near $M = 1$ and $M = 0$.

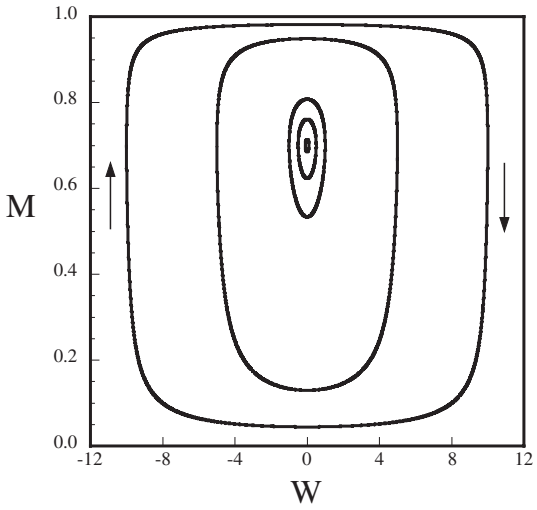

FIG. 4. *Orbits in the phase plane* (W, M) *obtained numerically from* (18)–(20). *The values of the parameters are* $v_2 = 0.5$, $V_{M3} = 1$, $V_{M4} = 0.7$, $v_d = 0.25$, $k_1 = k_2 = 1$, $K_c = 0.5$. *Each orbit corresponds to a periodic solution starting from a different initial point.* $M(0) = V_4/V_{M3} = 0.7$ *and* $W(0) = -0.1, -1, -5, -10$ *from the smallest to the largest orbit. The arrows indicate the direction of the time evolution.*

We now select the orbit of period P in the family of periodic solutions of (18) and (19). It is denoted by $U = U_P(T)$, $W = W_P(T)$, and $M = M_P(T)$. In order to determine how the period P (or equivalently, $U_P(T)$, $W_P(T)$, and $M_P(T)$) changes as we change a parameter, a higher order analysis is needed. This analysis is detailed in Appendix B. It leads to a solvability condition for bounded periodic solutions given by

$$v_d V_{M3} \frac{K_c}{(1-v_2)^2} \int_0^P \left(\frac{dM_P}{dT}\right)^2 dT - k_d \int_0^P \left(\frac{dU_P}{dT}\right)^2 dT = 0. \tag{22}$$

The two integrals must be computed numerically. This condition is the bifurcation equation since it relates the period of the oscillations and the physical parameters. In the limit of small amplitude solutions, $dU/dT = F'(M_0)dM/dT$, where $M_0 = V_4/V_{M3}$, and with $k_1 = k_2 = k$, (22) reduces to

$$\left[v_d V_{M3} \frac{K_c}{(1-v_2)^2} - k_d F'^2(M_0)\right] \int_0^P \left(\frac{dM_P}{dT}\right)^2 dT = 0 \tag{23}$$

which implies, using (20), that

$$k = k_H \equiv \sqrt{\frac{v_d V_{M3}}{k_d K_c}} \frac{(1-v_2)}{v_2} \left[\frac{1}{(1-M_0)^2} + \frac{1}{M_0^2}\right]^{-1}. \tag{24}$$

Using now $K = V_{M1}^{-1/2} k$ and $v_2 = V_2/V_{M1}$, expression (24) exactly matches the expression of the Hopf bifurcation point (47) obtained from the linearized theory in Appendix A. The expression (47) also is in excellent agreement with the exact numerical Hopf bifurcation line shown in Figure 3. We have thus verified that the bifurcation equation (22) correctly leads to the Hopf bifurcation point in the limit of small amplitude periodic solutions.

We next wish to find from (18)–(22) how the amplitude of the oscillations changes as we change the deviation $k - k_H$. To this end, we introduce

$$W = \sqrt{k}w \text{ and } T = \sqrt{k}s \tag{25}$$

into (18), (19) and obtain two equations for M and w that do not depend on k. They are of the form

$$f'(M)\frac{dM}{ds} = -v_d w, \tag{26}$$

$$\frac{dw}{ds} = V_{M3}M - V_4, \tag{27}$$

where

$$f(M) \equiv \frac{K_c v_2}{(1-v_2)^2}\left[\frac{1}{(1-M)} - \frac{1}{M}\right]. \tag{28}$$

Furthermore, substituting (25) into the bifurcation equation (22) leads to an expression for k^2 given by

$$k^2 = \frac{v_d V_{M3} K_c}{k_d(1-v_2)^2} \frac{\int_0^P \left(\frac{dM_P}{ds}\right)^2 ds}{\int_0^P f'^2(M)\left(\frac{dM_P}{ds}\right)^2 ds}. \tag{29}$$

The bifurcation equation (29) is now ready to be solved numerically: k appears only in the left-hand side, and the right-hand side is a function of the amplitude of the solution. Practically, we determine a P-periodic solution of (26) and (27) using the initial conditions

$$M(0) = V_4/V_{3M} \text{ and } w(0) = E, \tag{30}$$

where E is the parameter (in Figure 4, the orbits of different solutions are shown for $E = -0.1$, -1, -5, and -10). We then compute the two integrals in (29) and evaluate k^2. From an analysis of (27) and (27) in the phase plane, we note that $w = \pm E$ are the two extrema of $w(s)$. By gradually changing E from zero, we determine the function $E = E(k^2)$. Knowing E, we determine the extrema of W and X using first (25) and then (16). The bifurcation diagram of the extrema of X is shown in Figure 5 by the full lines. As the amplitude of the periodic solutions increases, the Hopf bifurcation branch is first subcritical ($K > K_H$) and then folds back.

4. Discussion. The QSSA is widely used in the study of oscillations in biological and physical systems as a means to analyze limit-cycle behavior in the phase plane. Focusing on a biochemical model for limit-cycle oscillations in the embryonic cell cycle, we showed that a routine application of the QSSA leads to a two-variable system of equations that does not exhibit sustained oscillations. This apparent failure of the QSSA is, however, not a limitation of the method. We need to remember that the QSSA originates from an asymptotic method that considers a specific limit of a parameter (here the limit $V_{M1} = V$ large assuming V_2/V_{1M} fixed). From the Hopf bifurcation conditions, we showed that periodic solutions can be found only in the full system if we consider small values of the Michaelis constants. The correct scaling between these parameters and the other parameters in the model is provided by a careful analysis of the Hopf bifurcation conditions. A nonlinear analysis motivated by

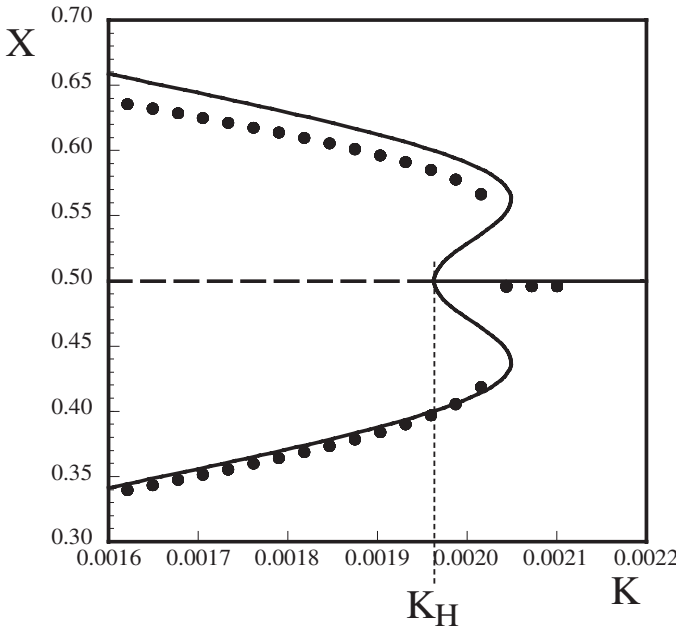

FIG. 5. *Maximum and minimum of the oscillations in X as a function of K. The approximation of the bifurcation diagram (full lines) is compared to the bifurcation diagram of the original evolution equations* (1)–(3) *(dots). Parameter values are the same as in Figure* 4. *We represent the extrema of X as a function of K. The horizontal line is the steady state $X = 0.5$ which is unstable if $K < K_H \simeq 1.963 \times 10^{-3}$. The value of $\varepsilon = 0.135$. The agreement becomes better if we consider smaller values of ε (i.e., higher values of V_{M1} and V_2).*

these scalings then leads to a two-variable problem as the leading approximation. This problem admits conservative oscillations and therefore does not provide the bifurcation diagram of the amplitude of limit-cycle oscillations as a function of the control parameter. A higher order analysis was necessary in order to derive the bifurcation diagram. In other words, the limit-cycle solution is captured by a two-variable problem as one particular orbit in a family of periodic solutions, but the relation of this orbit to a specific value of the control parameter requires an extra solvability condition. In the strict spirit of the QSSA, the technique, even corrected by taking into account the scaling between parameters, is unable to provide a two-variable system exhibiting limit-cycle oscillations. However, it is not a limitation of the singular perturbation method, which tell us how to rescue the QSSA by supplementing it with a solvability condition.

Our results came from investigating two orders of a perturbation analysis after scaling parameters and variables with respect to a small parameter ε. It is not a local analysis near a Hopf bifurcation point because M is arbitrary even if C and X are assumed close to their steady-state values. This is why we obtained the global bifurcation diagram in Figure 5. An alternative to the perturbation theory is possible if we directly introduce the new variables T, U, and W into the original equations (1)–(3). Inserting (16) into (13)–(15) and simplying, we obtain the following equations for U, M, and W:

$$\frac{dU}{dT} = -v_d W - \varepsilon k_d U, \tag{31}$$

$$\frac{dM}{dT} = \varepsilon^{-1}\left[\begin{array}{c}\frac{U(1-v_2)^2(1-M)-v_2\left(K_c+\varepsilon^2U(1-v_2)\right)k_1}{(K_c+\varepsilon^2U(1-v_2))(1-M+\varepsilon^2k_1)}\\ +\ \frac{v_2k_2}{M+\varepsilon^2k_2}\end{array}\right], \tag{32}$$

$$\frac{dW}{dT} = V_{M3}\frac{M(1-X_0-\varepsilon W)}{1-X_0-\varepsilon W+\varepsilon^2k_3} - V_4\frac{X_0+\varepsilon W}{X_0+\varepsilon W+\varepsilon^2k_4}, \tag{33}$$

where X_0 is defined in (17). The ε^{-1} term multiplying the right-hand side of (32) suggests that M will quickly approach a two-dimensional slow manifold. In this paper, we concentrated on the limit-cycle solution and didn't investigate the evolution towards this slow manifold.

The standard QSSA failed in our three-variable model because the small parameter that motivated the elimination of one of the dependent variables also controlled the time scale of the remaining variables. This problem is known for two-variable models exhibiting relaxation oscillations [20] and for the standard laser rate equations [22]. A change of variables allows us to eliminate the singular perturbation difficulty. For three-variable systems, the problem has been analyzed for laser dynamical systems [23, 24, 25].

Appendix A. Linear theory. The Hopf bifurcation boundaries were investigated only numerically [30, 31]. In this appendix, we determine analytically the steady-state solution of (1)–(3) and its Hopf bifurcation point for the particular case when

$$K_d = 0 \text{ and } K_j = K \ (j = 1-4). \tag{34}$$

The steady-state solution $(C, M, X) = (C_s, M_s, X_s)$ satisfies the following three conditions:

$$v_i - v_dX - k_dC = 0, \tag{35}$$

$$\frac{V_{M1}C}{K_c+C}\frac{1-M}{K+1-M} - \frac{V_2M}{K+M} = 0, \tag{36}$$

$$V_{M3}M\frac{1-X}{K+1-X} - V_4\frac{X}{K+X} = 0. \tag{37}$$

If $K \to 0$, the steady state (C_s, M_s, X_s) approaches the limit (C_0, M_0, X_0). From (35)–(36) with $K = 0$, we find

$$C_0 = \frac{K_cV_2}{V_{M1}-V_2} > 0,\ M_0 = \frac{V_4}{V_{M3}},\ \text{and}\ X_0 = \frac{v_i-k_dC_0}{\nu_d} > 0. \tag{38}$$

Introducing the deviations $u = C - C_s$, $v = M - M_s$, and $w = X - X_s$, the linearized problem is given by

$$\left(\begin{array}{c}u'\\v'\\w'\end{array}\right) = \left(\begin{array}{ccc}-k_d & 0 & -v_d\\ \frac{V_{M1}K_c}{(K_c+C)^2}\frac{1-M}{K+1-M} & -F_1 & 0\\ 0 & V_{M3}\frac{1-X}{K+1-X} & -F_2\end{array}\right)\left(\begin{array}{c}u\\v\\w\end{array}\right), \tag{39}$$

where we have omitted the subscript s for the steady state. F_1 and F_2 are positive coefficients defined by

$$\begin{aligned} F_1 &\equiv K\left[\frac{C}{K_c+C}\frac{V_{M1}}{(K+1-M)^2} + \frac{V_2}{(K+M)^2}\right],\\ F_2 &\equiv K\left[\frac{V_{M3}M}{(K+1-X)^2} + \frac{V_4}{(K+X)^2}\right]. \end{aligned} \tag{40}$$

From (39), we formulate the characteristic equation for the growth rate σ as

$$\sigma^3 - T_1\sigma^2 + T_2\sigma - T_3 = 0, \tag{41}$$

where

$$\begin{aligned} T_1 &= -k_d - F_1 - F_2, \\ T_2 &= k_d(F_1 + F_2) + F_1F_2, \\ T_3 &= -k_dF_1F_2 - V_{M3}V_{M1}v_d\frac{1-X}{K+1-X}\frac{K_c}{(K_c+C)^2}\frac{1-M}{K+1-M}. \end{aligned} \tag{42}$$

The conditions for a Hopf bifurcation are obtained by substituting $\sigma = i\omega$ into (41) and by separating the real and imaginary parts. We find

$$T_1T_2 - T_3 = 0 \text{ and } \sigma^2 = T_2 > 0. \tag{43}$$

The second condition is always verified. In order to satisfy the first condition, we determine $T_1T_2 - T_3$ and obtain

$$\begin{aligned} T_1T_2 - T_3 = &-k_d^2(F_1+F_2) - k_d(F_1+F_2)^2 - (F_1+F_2)F_1F_2 \\ &+ V_{M3}V_{M1}v_dK_c\frac{1-X}{K+1-X}\frac{1}{(K_c+C)^2}\frac{1-M}{K+1-M}. \end{aligned} \tag{44}$$

We wish to determine an approximation of (44) in the double limit K small and V large (V_{M1}/V_2 fixed). To this end, we need the leading expressions of F_1 and F_2 for K small. From (40) and using (38), we obtain

$$F_1 \simeq V_2K\left(\frac{1}{(1-M_0)^2} + \frac{1}{M_0^2}\right) \text{ and } F_2 \simeq V_4K\left(\frac{1}{(1-X_0)^2} + \frac{V_4}{X_0^2}\right). \tag{45}$$

We next consider the limit V_2 large (V_{M1}/V_2 fixed). In this limit, $F_1 \gg F_2$ and (44) simplifies as

$$\begin{aligned} T_1T_2 - T_3 &\simeq -k_dF_1^2 + V_{M3}V_{M1}v_d\frac{K_c}{(K_c+C_0)^2} \\ &= \left[\begin{array}{c} -k_dV_2^2K^2\left(\frac{1}{(1-M_0)^2} + \frac{1}{M_0^2}\right)^2 \\ + V_{M3}v_d\frac{(V_{M1}-V_2)^2}{K_cV_{M1}} \end{array}\right], \end{aligned} \tag{46}$$

where we eliminate C_0 using (38). The Hopf bifurcation point satisfies the condition $T_1T_2 - T_3 = 0$. Using (46) we find an expression of the Hopf bifurcation point $K = K_H$ given by

$$K_H = \frac{(V_{M1}-V_2)}{V_2\sqrt{V_{M1}}}\sqrt{\frac{V_{M3}v_d}{k_dK_c}}\left[\frac{1}{(1-M_0)^2} + \frac{1}{M_0^2}\right]^{-1}. \tag{47}$$

We have verified that this approximation compares well with the exact numerical solution shown in Figure 3. From (47), K_H scales like $V^{-1/2}$ as $V \to \infty$ ($V \equiv V_{M1}$, V_2/V_{M1} fixed). We also note from (43) that the frequency of the oscillations scales like

$$\omega = \sqrt{T_2} \simeq \sqrt{k_dF_1} = O(\sqrt{V_2K}) = O(V^{1/4}). \tag{48}$$

We conclude that a Hopf bifurcation is possible in the quasi-steady-state limit $V = V_{M1} \to \infty$ (V_2/V_{M1} fixed) provided that K is sufficiently small. The steady-state solution is unstable if $T_1T_2 - T_3 < 0$, which implies the inequality $K < K_H$.

Appendix B. Nonlinear bifurcation theory. Our starting point is (13)–(15), which we rewrite as

$$\frac{dC}{dT} = \varepsilon \left[v_i - v_d X \frac{C}{K_d + C} - k_d C \right], \tag{49}$$

$$\varepsilon^3 \frac{dM}{dT} = \frac{C}{K_c + C} \frac{1 - M}{\varepsilon^2 k_1 + 1 - M} - v_2 \frac{M}{\varepsilon^2 k_2 + M}, \tag{50}$$

$$\frac{dX}{dT} = \varepsilon \left[V_{M3} M \frac{1 - X}{\varepsilon^2 k_3 + 1 - X} - V_4 \frac{X}{\varepsilon^2 k_4 + X} \right] \tag{51}$$

so that all power of ε are positive. We next seek a periodic solution of the form

$$\begin{gathered} C = C_0 + \varepsilon C_1 + \varepsilon^2 C_2 + \cdots,\ M = M_0 + \varepsilon M_1 + \varepsilon^2 M_2 + \cdots, \\ \text{and } X = X_0 + \varepsilon X_1 + \varepsilon^2 X_2 + \cdots . \end{gathered} \tag{52}$$

After introducing (52) into (49)–(51), we equate to zero the coefficients of each power of ε. This leads to a sequence of problems for the coefficients in (52). The leading order equations are

$$\frac{dC_0}{dT} = 0,\ \frac{C_0}{K_c + C_0} - v_2 = 0,\ \frac{dX_0}{dT} = 0. \tag{53}$$

Equation (53) admits the solution

$$C_0 = \frac{K_c v_2}{1 - v_2} \text{ and } X_0 = cst, \tag{54}$$

where X_0 is an unknown constant. The fact that X_0 and M_0 are unknown motivates the higher order analysis. The next problem is $O(\varepsilon)$ and is given by the following three equations:

$$\frac{dC_1}{dT} = v_i - v_d X_0 \frac{C_0}{K_d + C_0} - k_d C_0, \tag{55}$$

$$\frac{K_c C_1}{(K_c + C_0)^2} = 0, \tag{56}$$

$$\frac{dX_1}{dT} = V_{M3} M_0 - V_4. \tag{57}$$

From (56) and then from (55), we find C_1 and X_0 as

$$C_1 = 0 \text{ and } X_0 = \frac{(v_i - k_d C_0)(K_d + C_0)}{v_d C_0}. \tag{58}$$

We have determined X_0 but M_0 is still unknown. Thus, we consider the next problem, which is $O(\varepsilon^2)$:

$$\frac{dC_2}{dT} = -v_d \frac{C_0}{K_d + C_0} X_1, \tag{59}$$

$$\frac{K_c C_2}{(K_c + C_0)^2} - \frac{C_0}{K_c + C_0} \frac{k_1}{1 - M_0} + v_2 \frac{k_2}{M_0} = 0, \tag{60}$$

$$\frac{dX_2}{dT} - V_{M3} M_1 = 0. \tag{61}$$

From (60), we may determine M_0 as a function of C_2. Specifically, we define $M_0 = G(C_2)$ as the implicit solution of

$$C_2 = F(M_0) = \frac{K_c v_2}{(1-v_2)^2}\left[\frac{k_1}{1-M_0} - \frac{k_2}{M_0}\right]. \tag{62}$$

From (57) and (59), we eliminate X_1 and formulate a second-order differential equation for C_2:

$$\frac{d^2C_2}{dT^2} + \frac{v_d C_0}{K_d + C_0}\left[V_{M3}G(C_2) - V_4\right] = 0. \tag{63}$$

This equation is conservative and admits a one-parameter family of periodic solutions. This can be demonstrated in the phase plane by determining a first integral. The conservative nature of the oscillations means that the amplitude is arbitrary, and we still need to examine the higher order problem.

An equation for X_2 is already given by (61). From the $O(\varepsilon^3)$ equations, we obtain equations for C_3 and M_1 given by

$$\frac{dC_3}{dT} = -v_d X_2 \frac{C_0}{K_d + C_0} - v_d X_0 \frac{K_d}{(K_d + C_0)^2} C_2 - k_d C_2 \tag{64}$$

and

$$\frac{dM_0}{dT} = \frac{K_c C_3}{(K_c + C_0)^2} - \frac{C_0}{K_c + C_0}\frac{k_1 M_1}{(1-M_0)^2} - v_2 \frac{k_2 M_1}{M_0^2}. \tag{65}$$

Using (65), we determine M_1 as

$$M_1 = G'(C_2)C_3 - \frac{K_c}{(1-v_2)^2} G'(C_2)^2 \frac{dC_2}{dT}. \tag{66}$$

Then, using (61), (64), and (66), we obtain

$$\begin{aligned}\frac{d^2C_3}{dT^2} + v_d \frac{C_0}{K_d + C_0} V_{M3} G'(C_2) C_3 = v_d \frac{C_0}{K_d + C_0} V_{M3} \frac{K_c}{(1-v_2)^2} G'(C_2)^2 \frac{dC_2}{dT} \\ - \left[v_d X_0 \frac{K_d}{(K_d + C_0)^2} + k_d\right] \frac{dC_2}{dT}.\end{aligned} \tag{67}$$

By differentiating (63) with respect to T, we note that the homogeneous linear problem for C_3 admits the solution $C_{3H} = dC_2/dT$. The condition for a bounded periodic solution then implies that the right-hand side of (67) satisfies a solvability condition (Fredholm alternative [32]). Because the homogeneous problem is self-adjoint, this condition requires that the right-hand side is orthogonal to C_{3H}. This leads to the integral

$$\int_0^P \begin{bmatrix} v_d \frac{C_0}{K_d + C_0} V_{M3} \frac{K_c}{(1-v_2)^2} G'(C_2)^2 \\ - \left(v_d X_0 \frac{K_d}{(K_d + C_0)^2} + k_d\right) \end{bmatrix} \left(\frac{dC_2}{dT}\right)^2 dT = 0 \tag{68}$$

and is the bifurcation equation. This equation can be further simplified, noting that

$$G'(C_2)^2 \left(\frac{dC_2}{dT}\right)^2 = \left(\frac{dM_0}{dT}\right)^2. \tag{69}$$

Equation (68) is then reformulated as

$$\int_0^P \left[\begin{array}{c} v_d \frac{C_0}{K_d+C_0} V_{M3} \frac{K_c}{(1-v_2)^2} \left(\frac{dM_0}{dT}\right)^2 \\ - \left(v_d X_0 \frac{K_d}{(K_d+C_0)^2} + k_d \right) \left(\frac{dC_2}{dT}\right)^2 \end{array} \right] dT = 0. \tag{70}$$

This condition determines the amplitude of the oscillations as a function of the physical parameters. If $K_d = 0$, it reduces to condition (22), which is analytically and numerically investigated.

REFERENCES

[1] J. D. Murray, *Mathematical Biology*, 3rd ed., Springer, New York, 2002.

[2] J. Keener and J. Sneyd, *Mathematical Physiology*, Interdiscip. Appl. Math. 8, Springer-Verlag, New York, 1998.

[3] C. P. Fall, E. S. Marland, J. M. Wagner, and J. J. Tyson, eds., *Computational Cell Biology*, Springer-Verlag, New York, 2002.

[4] L. A. Segel, *On the validity of the steady state assumption of enzyme kinetics*, Bull. Math. Biol., 50 (1988), pp. 579–593.

[5] L. A. Segel and M. Slemrod, *The quasi-steady-state assumption: A case study in perturbation*, SIAM Rev., 31 (1989), pp. 446–477.

[6] J. A. M. Borghans, R. J. De Boer, and L. A. Segel, *Extending the quasi-steady state approximation by changing variables*, Bull. Math. Biol., 58 (1996), pp. 43–63.

[7] C. C. Lin and L. A. Segel, *Mathematics Applied to Deterministic Problems in the Natural Sciences. With Material on Elasticity by G. H. Handelman*, 2nd ed., Classics Appl. Math. 1, SIAM, Philadelphia, 1988.

[8] I. R. Epstein and J. A. Pojman, *An Introduction to Nonlinear Chemical Dynamics*, Oxford University Press, Oxford, UK, 1998.

[9] A. Goldbeter, *Models for oscillations and excitability in biological systems*, in Mathematical Models in Molecular and Cellular Biology, L. A. Segel, ed., Cambridge University Press, Cambridge, UK, 1980, pp. 248–291.

[10] A. Goldbeter, T. Erneux, and L. A. Segel, *Excitability in the adenylate cyclase reaction in Dictyostelium discoideum*, FEBS Lett., 89 (1978), pp. 237–241.

[11] A. Goldbeter, *Biochemical Oscillations and Cellular Rhythms*, Cambridge University Press, Cambridge, UK, 1996.

[12] A. Goldbeter and D. E. Koshland, Jr., *An amplified sensitivity arising from covalent modification in biological systems*, Proc. Nat. Acad. Sci. U.S.A., 78 (1981), pp. 6840–6844.

[13] L. A. Segel and A. Goldbeter, *Scaling in biochemical kinetics: Dissection of a relaxation oscillator*, J. Math. Biol., 32 (1994), pp. 147–160.

[14] L. Holden and T. Erneux, *Slow passage through a Hopf bifurcation: From oscillatory to steady state solutions*, SIAM J. Appl. Math., 53 (1993), pp. 1045–1058.

[15] L. Holden and T. Erneux, *Understanding bursting oscillations as periodic slow passages through bifurcation and limit points*, J. Math. Biol., 31 (1993), pp. 351–365.

[16] A. Goldbeter, *A minimal cascade model for the mitotic oscillator involving cyclin and cdc2 kinase*, Proc. Nat. Acad. Sci. U.S.A., 88 (1991), pp. 9107–9111.

[17] A. Goldbeter, *Modeling the mitotic oscillator driving the cell division cycle*, Comments in Theoret. Biol., 3 (1993), pp. 75–.

[18] J. J. Tyson, A. Csikasz-Nagy, and B. Novak, *The dynamics of cell cycle regulation*, BioEssays, 24 (2002), pp. 1095–1109.

[19] T. Erneux, R. D. Edstrom, and A. Goldbeter, *Enzyme sharing in phosphorylation-dephosphorylation cascades: The case where one protein kinase (or phosphatase) acts on two different substrates*, J. Theoret. Biol., 165 (1993), pp. 43–61.

[20] S. M. Baer and T. Erneux, *Singular Hopf bifurcation to relaxation oscillations*, SIAM J. Appl. Math., 46 (1986), pp. 721–739.

[21] G. J. Merchant, R. J. Braun, K. Brattkus, and S. H. Davis, *Pulsatile instability in rapid directional solidification: Strongly-nonlinear analysis*, SIAM J. Appl. Math., 52 (1992), pp. 1279–1302.

[22] G.-L. Oppo and A. Politi, *Toda potentials in laser equations*, Z. Phys. B, 59 (1985), pp. 111–115.

[23] G.-L. Oppo and A. Politi, *Center-manifold reduction for laser equations with detuning*, Phys. Rev. A (3), 40 (1989), pp. 1422–1427.
[24] T. Erneux and G. Kozyreff, *Nearly vertical Hopf bifurcation for a passively Q-switched microchip laser*, J. Statist. Phys., 101 (2000), pp. 543–552.
[25] G. Kozyreff and T. Erneux, *Singular Hopf bifurcation to strongly pulsating oscillations in lasers containing a saturable absorber*, European J. Appl. Math., 14 (2003), pp. 407–420.
[26] A. C. Fowler, *Mathematical Models in the Applied Sciences*, Cambridge Texts Appl. Math., Cambridge University Press, Cambridge, UK, 1997.
[27] P. C. Engel, *Enzyme Kinetics*, John Wiley & Sons, New York, 1977.
[28] H. Haken, *Synergetics*, 3rd ed., Springer, Berlin, 1983.
[29] S. H. Strogatz, *Nonlinear Dynamics and Chaos*, Addison-Wesley, New York, 1995.
[30] P. C. Romond, J. M. Guilmot, and A. Goldbeter, *The mitotic oscillator: Temporal self-organization in a phosphorylation-dephosphorylation enzymatic cascade*, Ber. Bunsenges. Phys. Chem., 98 (1994), pp. 1152–1159.
[31] A. Goldbeter and J.-M. Guilmot, *Thresholds and oscillations in enzymatic cascades*, J. Phys. Chem., 100 (1996), pp. 19174–19181.
[32] G. Iooss and D. D. Joseph, *Elementary Stability and Bifurcation Theory*, Undergrad. Texts Math., Springer-Verlag, New York, 1980, 2nd ed., Springer, New York, 1990.